Research on Rigid Body Motion Tracing in Space based on NX MCD

Junjie Wang[1], Chunxiang Dai[1] , Karen Shi[2] and Rongkang Qin[1]

[1] Mechanical Manufacturing and Automation Institute, Shanghai University, No.149 YanChang Road, Shanghai, China
[2] SIEMENS Product Lifecycle Management Software Inc., No.1018 ChangNing Road, Shanghai, China

Abstract. In the use of MCD (Mechatronics Concept Designer) which is a module belong to SIEMENS Ltd industrial design software UG (Unigraphics NX), user can define rigid body and kinematic joint to make objects move according to the existing plan in simulation. At this stage, user may have the desire to see the path of some points in the moving object intuitively. In response to this requirement, this paper will compute the pose through the transformation matrix which can be available from the solver engine, and then fit these sampling points through B-spline curve. Meanwhile, combined with the actual constraints of rigid bodies, the traditional equal interval sampling strategy was optimized. The result shown that this method could satisfy the demand and make up for the deficiency in traditional sampling method. User can still edit and model on this 3D curve. Expected result has been achieved.
Keywords. MCD; simulation; path; sampling strategy.

1. Introduction

In 1970s, the concept of Mechatronics was formally introduced, many design ideas have been applied to this. And Conceptual Design is a process from simple to precise, fuzzy to clear, combining Mechatronics and Conceptual Design can make the project more flexible [1][2]. SIEMENS is involved deeply in the field of Mechatronics Conceptual Design. The research of this paper was based on MCD (Mechatronics Concept Designer) which is a module of SIEMENS industrial design software UG NX. In the design process, consider from completing the task, drive and actuation mechanism is the core of the machine. Therefore, in the simulation of the conceptual model, users are concerned about the path of these two mechanisms [3][4]. This paper will aim at the requirement of tracing the path of the actuator in models, realize it through real time calculation of actuators' position and fitting of these result points. Meanwhile, this paper proposed an optimized sampling method which would first analyze the restrained condition of actuators. Experimental results show that this method can fit well to the path and make up for the deficiency in traditional sampling method.

2. Method

2.1 Transform Matrix

In computer, graphics are processed in the form of numbers [5]. To change the position of a point, a commonly used method is to multiply the coordinate value with a 4×4 transformation matrix. It can make any point move to another position through adjusting the parameters in this matrix. The formula is

$$(x' \quad y' \quad z' \quad 1) = (x \quad y \quad z \quad 1) \cdot \begin{pmatrix} M_{11} & M_{12} & M_{13} & M_{14} \\ M_{21} & M_{22} & M_{23} & M_{24} \\ M_{31} & M_{32} & M_{33} & M_{34} \\ M_{41} & M_{42} & M_{43} & M_{44} \end{pmatrix} \tag{1}$$

Let $M_{rot} = \begin{pmatrix} M_{11} & M_{12} & M_{13} \\ M_{21} & M_{22} & M_{23} \\ M_{31} & M_{32} & M_{33} \end{pmatrix}$.

The 3×3 matrix $\mathrm{M_{rot}}$ controls the basic transformation of the proportion, symmetry and rotation in 3D graphics. The physics engine will convert the position or speed constraint into force and torque, and decompose equivalently into direction of each axis. In this way, the rotation matrix can be obtained in real time calculation. Thus, the matrix can be divided into

$$M_{rot} = M_z(\varphi)M_y(\gamma)M_x(\theta) .$$

$M_a(\delta)$ represents the rotation of δ degrees around the ***a*** axis.

$(M_{41} \quad M_{42} \quad M_{43})$ controls the transformation along the coordinate axis. The solution method is similar to rotation matrix.

However, in MCD kinematics simulation environment [6], it does not involve the transformation of size, perspective, and graphics scale. So in the process of calculation, $(M_{14} \quad M_{24} \quad M_{34})^T$ which controls the transformation of perspective equals to $(0 \quad 0 \quad 0)^T$. And M_{44} which controls the size and scale transformation equals to 1.

2.2 Theoretical Derivation & Formula

The pose change of a rigid body in space can be decomposed into translational motion and rotation. In practical engineering problems, two characteristics of rigid body are often adopted. First, and equal in translation. Second, the displacement, velocity and acceleration of each mass element in a rigid body are the same [7].

In this paper, the translational motion is simplified as the coordinate change of the mass point M of this rigid body. And the rotation is simplified as the change of the vector $\overrightarrow{MA}$ which is the difference between M and selected point A which is belong to this rigid body.

In the implementation, each solution achieved by engine called Step, and each step would generate a corresponding 4×4 matrix. Noted that some elements in the matrix equal to 0 or 1, so it was better to calculate the coordinates through motion synthesis instead of multiplying them directly.

Set coordinate value of the sampling point A as (x y z), and the mass center M of this rigid body as $(\mathrm{m}_x \ \mathrm{m}_y \ \mathrm{m}_z)$, point O is the origin. After the rigid body starts to move, the position will change. Now we will set the mass point M_i as $(\mathrm{m}_{xi} \ \mathrm{m}_{yi} \ \mathrm{m}_{zi})$, and set the point A_i (i means step i) as $(\mathrm{m}_{xi} \ \mathrm{m}_{yi} \ \mathrm{m}_{zi})$. Then the formula for A_i is

$$\overrightarrow{\mathrm{OA}_i} = \overrightarrow{O\mathrm{M}_i} + \overrightarrow{M_iA_i} \tag{2}$$

$$\text{Means } \overrightarrow{\mathrm{OA}_i} = \overrightarrow{O\mathrm{M}_i} + \overrightarrow{MA} \cdot \begin{pmatrix} M_{11} & M_{12} & M_{13} \\ M_{21} & M_{22} & M_{23} \\ M_{31} & M_{32} & M_{33} \end{pmatrix}.$$

$$\text{The result is } \begin{pmatrix} x_i \\ y_i \\ z_i \end{pmatrix} = \begin{pmatrix} m_{xi} + M_{11} \cdot (x - m_x) + M_{21} \cdot (y - m_y) + M_{31} \cdot (z - m_z) \\ m_{yi} + M_{12} \cdot (x - m_x) + M_{22} \cdot (y - m_y) + M_{32} \cdot (z - m_z) \\ m_{zi} + M_{13} \cdot (x - m_x) + M_{23} \cdot (y - m_y) + M_{33} \cdot (z - m_z) \end{pmatrix}. \tag{3}$$

In this formula, $\begin{pmatrix} m_{x_i} \\ m_{y_i} \\ m_{z_i} \end{pmatrix} = \begin{pmatrix} m_{x_{i-1}} + M_{41} \\ m_{y_{i-1}} + M_{42} \\ m_{z_{i-1}} + M_{43} \end{pmatrix}$.

2.3 User Interface & Data Structure

User interface is shown in the figure 1, and the parameters are shown in the Table 1.

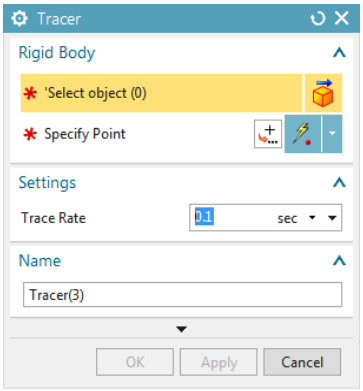

Figure 1. User Interface of Tracer.

Table 1. Parameters in User Interface.

Variable Name	Type	Specification
Select Object	rigid_body	Select a geometry as rigid body.
Specify Point	PNT_3	A point belong to this rigid body.
Tracer Rate	double	Set a rate (sec) of the trace.
Name	string	Set tracer's name.

After sampling an existing rigid body and specifying a point, the tracer will sample this point at intervals. And the trace rate can be also set by user. Then, the result will be calculated by (2).

2.4 Description & Analysis of the Fitting Strategy

A series of coordinate points could be obtained by the above calculation. In order to get the smooth curve, B-spline curve interpolation [8] is used to fit the sampling points [9][10].

Determining a spline curve requires the control point P, then in drawing, the points on the curve will be computed by recursion on the control polygon. For example, a set of points $C = \{c_j : j = 1,2,\dots,k\}$ is on a B-spline curve, so it should satisfied the definition of B-curve [11][12], which is

$$c_j(u_j) = \sum_{j=0}^{n} N_{j,p}(u_j) P_j,\ j = 1,2,\dots,k \cdot \tag{4}$$

The formula (4) can be written in matrix form, i.e. $C = NP$. P is a $n \times 3$ matrix with n control points unknown. C is a $k \times 3$ matrix with k 3D points. N is a $k \times n$ coefficient matrix which is the basis functions of the B-spline. If we input a series of points and determine the value of the node vector u, as a result, N can be calculated by de Boor's algorithm [11]. And finally, we can get the matrix P which will include the control points.

The application of B-spline in this paper would meet two special cases. First, the sampling points may lie on the same line in a rigid body motion. One of the properties of B-spline is convex hull property, it makes sure that B-spline should locate in the control polygon surrounding by the nodes. So it can make B-spline degenerate into a line if the control points lie on one line.

The other one is for filtration to multiple-knot. Rigid body may not move in a period of time, if using equal interval sampling, repeat points will be collected at this position. When generating, multiple same points will make the differentiability of the B-spline lower [12], that means will produce "sharp points". The path mentioned in this paper does not need to consider multiple-knot, so it should avoids the occurrence of this situation. Following conditions should be added after each calculation.

```
PNT_3 last_point = samplePointVec.back();   //get the last sample point
if ( last_point.distance (result_point) > 0.01)   //the distance between result point and last point should more than 0.01
    samplePointVec.push_back (result_point);  //insert this point
```

3. Optimization

3.1 Preparation for Optimizing

As the most basic sampling method, Equal Interval Sampling was used in many kinds of literature and also in this paper. Its advantage is that users only need to determine the tracer rate, through condition

$$\text{if } (\,(++\text{step})\%\ (1000 \times \text{tracer\_rate}) == 0\,)$$

to determine whether matrix calculation should be performed. It has less computation frequency and less memory consumption. However, it has obvious deficiencies in using just like the figure 2 and figure 3. There is little nuance between the two, but the amount of calculation is ten times difference.

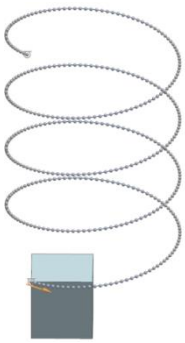

Figure 2. A path line of a block with 0.1ms as trace rate.

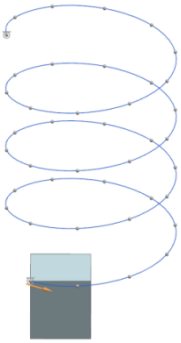

Figure 3. A path line of a block with 1ms as trace rate.

Also in the conceptual design, user can use “Line”, “Arc” and “Spline” which are the modelling command of NX to generate curves. Then they can use “Point on Curve Joint” which is the command of MCD to make the rigid body move along this curve. For example, user want to trace point A in the following mechanism shown in figure 4.

Figure 4. Mechanism for Point on Curve Joint Effects.

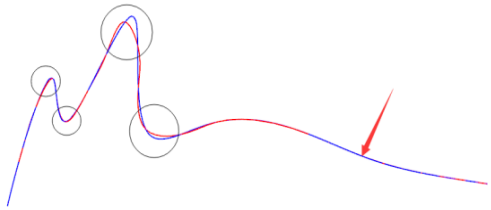

Figure 5. Comparison of Result Curves with Different Sampling Frequencies.
Red: 0.5 & Blue: 0.05

Sampling frequency was set 0.5 and 0.05 respectively, the results have been represented by a red line and a blue line. The figure 5 was the result of comparison.
In contrast, it is obvious that there is a significant fitting distortion in rings. At the arrow point, although great difference in the number of sampling points, the results are similar. In order to save the computational cost and achieve more accurate fitting in tracking, it is necessary to set a higher sampling frequency for the "critical" position of the curve.
Meanwhile in MCD, the joints are referenced on rigid bodies can be analysed. Sliding joint, hinge joint and cylindrical joint will make objects move with linear variation, so Equal Interval Sampling will be a better method for these cases. And when meet “Point on Curve Joint” or “Path Constraint Joint”, before sampling, this paper propose that it need to analysis the curve\path to get the critical position. Finally, *Equidistance Sampling Method* can be used for some nonlinear or composite joints situations.

3.2 Analyzing before Sampling
This paper considers that the curvature distribution of a curve can reflect its overall and local characteristics. Therefore, the sampling frequency needs to be related to this curve’s curvature distribution. Take figure 6 as an example to illustrate the method. The curve in the graph can be turn into discrete to get points, and the radius of curvature at the ith point can be calculated by the following formula,

$$\rho_i = \frac{\left|\overrightarrow{d_i d_{i+1}}\right|\left|\overrightarrow{d_i d_{i-1}}\right|\left|\overrightarrow{d_i d_{i+1}} - \overrightarrow{d_i d_{i-1}}\right|}{2 \times \left|\overrightarrow{d_i d_{i+1}} \times \overrightarrow{d_i d_{i-1}}\right|}. \quad (5)$$

The value of curvature is small. In order to facilitate calculation and explanation, the results are multiplied by 1000 times, so that it can be drawn in the integer category. The image is shown in the Fig 6,

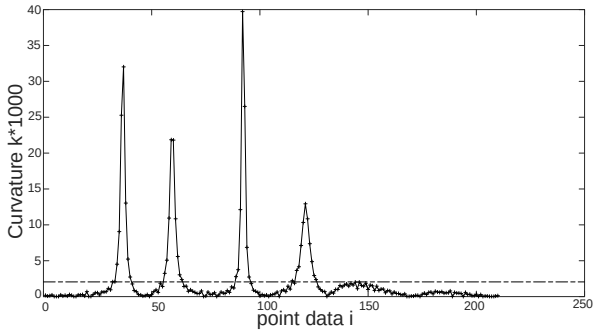

Figure 6. Curvature Distribution.

After the curvature data is obtained, the mean value $\bar{k}$ and overall standard deviations S should be calculated

$$\bar{\mathrm{k}} \approx 2.12,\ \mathrm{S} = \sqrt{\frac{1}{N}\sum_{i=1}^{N}(Xi - \bar{X})^2} \approx 5.11\ .$$

To determine the critical position, this paper designed a value K'. If it is larger than K', it represents this section as the key position. In order to maximize the response of key points and also can filter out the others, let $\mathrm{K}' = [\bar{\mathrm{k}}]$, which means integer to $\bar{\mathrm{k}}$.

The curvatures in the following four intervals C1[32, 40], C2[56, 64], C3[89, 95] and C4[115,126] are larger than K'. Their overall standard deviations are S1≈10.300, S2≈7.266, S3≈13.252 and S4≈3.614. And The curvatures in the following five intervals C_5[1, 31], C_6[41, 55], C_7[65, 88], C_8[96, 114] and C_9[126, 210] are smaller than K'. Their overall standard deviations are S_5≈0.294, S_6≈0.573, S_7≈ 0.400, S8≈0.480, S9≈0.559.

Since the overall standard deviation represents the degree of dispersion between data and mean, the greater the degree of discretization, the greater the variation of the curvatures. S1 to S4 are greater than 1, while the remaining S5 to S9 are less than 1, take S as a reference, this paper held that the intervals which curvature value is greater than K' and S_i is greater than 1 are the critical position. When the rigid body moves to the critical position, the sampling frequency set in this paper needs to refer to the maximum curvature of this interval,

$$R_i = \frac{1}{1000\times(k_{\max})_{ci}} = \frac{(\rho_{\min})_{ci}}{1000},\ \ R_{\min} \geq 0.001 \tag{6}$$

After a number of curve tests, the value of S should be less than 10, if greater than, it should not take the above method.

3.3 Equidistance Sampling Method

For the above conditions are not applicable and some complex cases, motion would be more inscrutability. The paper held that the amount of computation needed to be increased to pursue accuracy, so Equidistance Sampling Method performed better.

In the later stage of conceptual design, the motion of many rigid bodies is composed of complicated kinematic joints, such as a point on a connecting rod of a four-bar linkage, or some points in the manipulator's executing mechanism. While in the classical Curve Splitting algorithm [13], the sharp angle of the curve is used as the key frame, because the change between each sharp angle can be expressed linearly, but this algorithm is very heavy in calculation. Another is through the analysis of the rotation matrix.Since the rotation matrix can be decomposed into Euler Angle, through the analysis of angle change can also achieve the purpose. However, to trace the rotation center of a rotating object for example the center of mass of a drill bit. A large amount of calculation but the final result is of no significance.

$$\delta = 1/k \cdot 2^d \tag{7}$$

k represent the degree of accuracy

sampling result will be better. In practice, once this value is exceeded, this point should be record.

4. Result

It's reasonable to use Hausdorff [14] distance evaluation as the error evaluation. The fitting requirement of the data point cloud is that the distance between the fitted curve and the original data point cloud is within a certain tolerance range. The fitting curve of $P_i(i = 1, \dots, n)$ is $C(t)$, projected P_i onto $C(t)$ to get P'_i. The fitting error and average error are

$$e_i = \|P'_i - P_i\| \tag{8}$$

$$e_i = (\sum_{i=1}^{n} e_i^2)^{1/2}/n. \tag{9}$$

In this paper, the average error was used as the basis of judgment for the method which will analyse before sampling.

Take the mechanism in figure 6 as the experimental object of this method, the result is shown by the following figure 7.

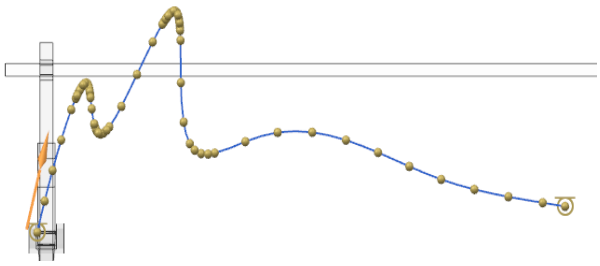

Figure 7. Result of the Method of Analyzing before Sampling.

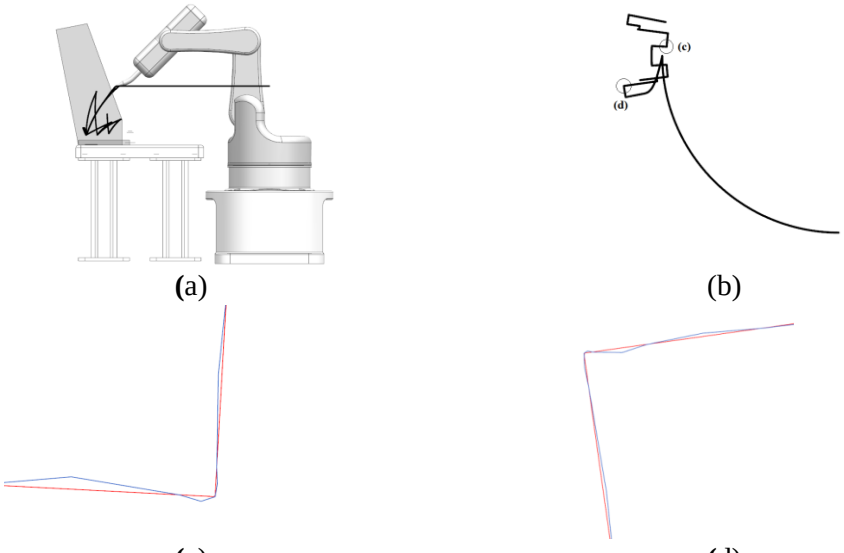

(a) (b)

(c) (d)

Figure 8. Result of the Equidistance Sampling Method.

Compared with equal interval sampling method with 0.03s as the tracking frequency, the optimization method used in this paper can be calculated less than 8400 times in point calculation. The average error between the two paths is 0.05283. When multiple tracers are installed at the same time, more computational costs can be saved.

Then by setting k=1, used *Equidistance Sampling Method* to generate the trajectory of a welding manipulator [15] in figure 10(a) which degree of freedom is 5. And used *Equal Interval Sampling* with the trace rate of 0.05s as contrast.

This paper used red to represent the result of Equal Interval Sampling method, blue to represent Equidistance method. In figure 8 (c) and figure 8 (d), maximum local fitting error of equal sampling method reached 0.164, while equidistance method only 0.009. Also, each cusp in the curve fitted by equidistance sampling method was better than by equal interval.

5. Summary

This paper realized the visual display of rigid body motion trajectory based on Mechatronics Concept Design. And also proposed two sampling optimization methods which are *Analyzing before Sampling Method* and *Equidistance Sampling Method*. The first method will analyse the curvature of constrained curves, determine sampling strategy according to the analysis result. Its advantage is the amount of computation can be reduced substantially with little accuracy loss. However, the curvature is hard to extract. *Equidistance Sampling Method* can give a more accurate result, but the amount of calculation is much larger than the other method. In the future research, how to combine the strategy of sampling and fitting more effectively can be a research direction.

6. References

[1] Yinli Jin, Jianpin Zhang and Kun Ye. 2013 Energy and Energy Conservation. *Parametric Modeling of Large Fan Blades based on NX Secondary Development.* chapter 6, pp. 133-135

[2] Jack Xiong, Chunxiang Dai and Karen Shi. 2016 Metrology & Measurement Technique. *Research and Application of NX mechatronic Concept Design System.* chapter 12, pp. 9-11

[3] A. Roennau, F. Sutter, G. Heppner, J. Oberlaender and R. Dillmann. 2013 16th International Conference on Advanced Robotics. *Evaluation of Physics Engines for Robotic Simulations with a Special Focus on the Dynamics of Walking Robots.* pp. 1-7

[4] Jianshe Guo, Biaoguang Sun and Yunpeng Zhang. 2011 Machinery. *Manual Mechanical Simulation of Punch Machine based on UG*. chapter 21, pp. 479

[5] Di Wu and Wenqian Huang. 2003 Hydrographic Surveying and Charting. *Deduction of Transformation Matrix of Perspective Projection in Graph Transformation.* chapter 23, pp. 18

[6] *PhysX by NVIDIA.* in Ver. 3.1, more details at: http://www.geforce.com/hardware/technology/physx website 2013.

[7] L. Glondu, M. Marchal, G. 2010 ASME Conference Proceedings. *Dumont, Evaluation of Physical Simulation Libraries for Haptic Rendering of Contacts between Rigid Bodies.*

[8] Rama Krishna N Parasaram and T N Charyulu. 2012 International Journal of Mechanical Engineering and Robotics Research. *Airfoil Profile Design by Reverse Engineering Bezier Curve.* Vol.1, No.3, pp. 410-420

[9] Yoshimoto F, Harada T, Yoshimoto Y. 2003 Computer-Aided Design. *Data fitting with a spline using a real-coded genetic algorithm*. chapter 35(8), pp 751-760.

[10] Kenneth Renny Simba, Naoki Uchiyama, and Shigenori Sano. 2016 Robotics and Computer-Integrated Manufacturing *Realtime smooth trajectory generation for nonholonomic mobile robots using bezier curves.* chapter 41, pp 31–42.

[11] *B-spline Definition & Introduction.* details and manual at: https://en.wikipedia.org/wiki/B-spline, website 2017.

[12] HAN Jiang, JIANG Ben-chi. 2010 Applied Mathematics and Mechanics. *A B-Spline Curve Fitting Algorithm Based on Contour Key Points.* chapter 36, pp. 423-431

[13] Hongmei Zhou, Yanming Wang. 2008 Journal of Xi'an Jiaotong University. *Fitting of non-uniform Rational B-spline Curves based on Minimum Control Points.* chapter 42, pp. 73-77

[14] Park H. 2004 Computer Aided Geometric Design. *An error-bounded approximate method for representing planar curves in B-splines.* chapter 1, pp. 9-12

[15] Harshal B Sonawane and Eknath R Deore. 2014 International Journal of Mechanical Engineering and Robotics Research. *Finite Element Model for the Effect of Heat Input & Speed on Residual Stress during Weldings.* Vol.3, No.3, July 2014